Molecular Biology of the Cell
Vol. 15, 3758–3770, August 2004

Rab22a Regulates the Recycling of Membrane Proteins Internalized Independently of Clathrin[V]

Roberto Weigert, Albert Chi Yeung, Jean Li, and Julie G. Donaldson*

Laboratory of Cell Biology, National Heart, Lung, and Blood Institute, National Institutes of Health, Bethesda, Maryland 20892-8017

Submitted April 27, 2004; Revised May 18, 2004; Accepted May 24, 2004
Monitoring Editor: Jean Gruenberg

Plasma membrane proteins that are internalized independently of clathrin, such as major histocompatibility complex class I (MHCI), are internalized in vesicles that fuse with the early endosomes containing clathrin-derived cargo. From there, MHCI is either transported to the late endosome for degradation or is recycled back to the plasma membrane via tubular structures that lack clathrin-dependent recycling cargo, e.g., transferrin. Here, we show that the small GTPase Rab22a is associated with these tubular recycling intermediates containing MHCI. Expression of a dominant negative mutant of Rab22a or small interfering RNA-mediated depletion of Rab22a inhibited both formation of the recycling tubules and MHCI recycling. By contrast, cells expressing the constitutively active mutant of Rab22a exhibited prominent recycling tubules and accumulated vesicles at the periphery, but MHCI recycling was still blocked. These results suggest that Rab22a activation is required for tubule formation and Rab22a inactivation for final fusion of recycling membranes with the surface. The trafficking of transferrin was only modestly affected by these treatments. Dominant negative mutant of Rab11a also inhibited recycling of MHCI but not the formation of recycling tubules, suggesting that Rab22a and Rab11a might coordinate different steps of MHCI recycling.

INTRODUCTION

Endocytosis encompasses a variety of processes that cells use to internalize plasma membrane proteins and lipids, and extracellular molecules. There are two main classes of endocytosis: clathrin-dependent and clathrin-independent (Nichols and Lippincott-Schwartz, 2001; Johannes and Lamaze, 2002; Conner and Schmid, 2003). Molecules traveling through the clathrin-dependent pathway are internalized via small endocytic vesicles coated by clathrin. After uncoating, the endosomal vesicles fuse with the early endosomal compartment and the itinerant proteins and lipids are either transported to the late endosomes/lysosomes to be degraded or recycled back to the plasma membrane (Gruenberg and Maxfield, 1995; Bonifacino and Traub, 2003; Maxfield and McGraw, 2004).

Clathrin-independent endocytosis ranges from pinocytosis to macropinocytosis and phagocytosis, which are stimulated, actin-driven processes (Watts, 1997; Aderem and Underhill, 1999; Chimini and Chavrier, 2000). We have shown that several molecules lacking the AP-2 localization signal, such as major histocompatibility complex class I (MHCI), the alpha-subunit of the interleukin-2 receptor (Tac), integrins, and GPI-anchored proteins, traffic through a clathrin-independent, Arf6-associated endocytic pathway (Radhakrishna and Donaldson, 1997; Brown *et al*., 2001; Naslavsky *et al*., 2003, 2004). Such molecules are internalized from the PM via nonclathrin-derived structures that subsequently fuse with the early endosomes containing clathrin-derived cargo proteins. From there, MHCI can proceed to the late endosomes/lysosomes for degradation or be recycled back to the plasma membrane (PM) independently from the cargo traveling through the clathrin-dependent pathways (Caplan *et al*., 2002; Naslavsky *et al*., 2003). Although many molecules have been identified and characterized as regulators of the clathrin-dependent pathway (Clague, 1998; Miaczynska and Zerial, 2002; Pfeffer, 2003), very little is known about the regulation of the clathrin-independent pathways. We reasoned that the machinery regulating processes such as sorting, fission, and fusion in the clathrin-independent pathway might share common elements with the clathrin-dependent pathway and involve molecules belonging to one of the class of proteins already shown to have a role in endocytosis, e.g., adaptors, coat proteins, soluble *N*-ethylmaleimide–sensitive factor attachment protein receptors, and, in particular, Rab GTPases.

Rab proteins are Ras-related GTPases that are key regulators in many steps of the endocytic process (Chavrier and Goud, 1999; Somsel Rodman and Wandinger-Ness, 2000; Segev, 2001; Seabra *et al*., 2002). Rab5 regulates the fusion of endocytic vesicles with early endosomes and regulates transport of early endosomes along microtubules (Nielsen *et al*., 2000; Zerial and McBride, 2001). Rab4 and Rab11 are involved in the recycling of clathrin cargo, such as transferrin receptor (TfnR), from the endosomes to the PM (van der Sluijs *et al*., 1992; Ullrich *et al*., 1996; Schlierf *et al*., 2000; de Wit *et al*., 2001). Recent findings suggest that Rab11a also may play a role in the recycling of nonclathrin-derived cargo back to the plasma membrane (Powelka *et al*., 2004). Rab7 is involved in trafficking from early endosomes to late endosomes/lysosomes (Press *et al*., 1998), and Rab 9 regulates trafficking from late endosomes to the *trans*-Golgi network (Lombardi *et al*., 1993; Barbero *et al*., 2002). Rab15 has been localized to clathrin-derived endosomes and regulates recycling (Zuk and Elferink, 2000), and, more recently, Rab22a

Article published online ahead of print. Mol. Biol. Cell 10.1091/mbc.E04–04–0342. Article and publication date are available at www.molbiolcell.org/cgi/doi/10.1091/mbc.E04–04–0342.
[V] Online version of this article contains supporting material. Online version is available at www.molbiolcell.org.
* Corresponding author. E-mail address: jdonalds@helix.nih.gov.

has been suggested to act at multiple levels in the endocytic pathway (Mesa *et al*., 2001; Kauppi *et al*., 2002).

In this study, we investigated whether any members of the Rab family would localize to or regulate the clathrin-independent/Arf6-associated endocytic pathway. We show that both endogenous and overexpressed Rab22a are localized on the MHCI-containing, recycling endosomal tubules that lack TfnR. Overexpression of Rab22a and mutants impaired in the GTP cycle inhibited recycling of MHCI to the PM, whereas trafficking of clathrin-dependent cargo proteins (e.g., transferrin, Tfn) was not affected. The inhibition of recycling correlated with alterations in the morphology of MHCI-containing endosomes. Furthermore, modulation of cellular levels of Rab22a achieved either by overexpression of Rab22a or by small interfering RNA (siRNA)-mediated depletion impaired the recycling of MHCI to the PM and affected the formation of tubular structures. Interestingly, overexpression of dominant negative mutants of Rab11a inhibited MHCI recycling to the PM without affecting the tubular morphology of the recycling intermediates. Our data indicate that Rab22a and Rab11a specifically regulate different steps in the recycling of cargo protein that has entered the cell independently of clathrin.

MATERIALS AND METHODS

Cells, Reagents, and Antibodies

HeLa, Cos7, and A431 cells were grown in DMEM as described previously (Brown *et al*., 2001), whereas Caco2 cells were grown under the same conditions but using Eagle's Minimum Essential Media. Latrunculin A (LatA) and saponin were from Sigma-Aldrich (St. Louis, MO). Mouse monoclonal antibody to human MHCI (W6/32) was described previously (Naslavsky *et al*., 2003). Cy3-conjugated anti-MHCI (W6/32) antibody was prepared with FluorolinkM antibody Cy3-labeling kit (Amersham Biosciences, Piscataway, NJ). Rabbit polyclonal antibody to Arf6 was described previously (Song *et al*., 1998). Monoclonal antibodies against Rab5, EEA1, and GM130 were from BD Biosciences (Palo Alto, CA). The polyclonal antibody against Rab4 used for immunofluorescence was a generous gift from Dr. Peter van der Sluijs (Utrecht University, Utrecht, The Netherlands). The affinity-purified rabbit polyclonal antibody against Rab4 used for immunoblotting was from Santa Cruz Biotechnology (Santa Cruz, CA). Rabbit polyclonal and mouse monoclonal antibodies directed against Rab11 and TfnR, respectively, were from Zymed Laboratories (South San Francisco, CA). Polyclonal antibody against actin was from Sigma-Aldrich. Tfn conjugated to Alexa 488, 594, and 633 and all secondary antibodies conjugated to 594, 488, and 647 were from Molecular Probes (Eugene, OR).

Plasmids and Transient Transfections

Green fluorescent protein (GFP)-Rab5, GFP-Rab4, GFP-Rab7, and their mutants were from Dr. R. Lodge (University of Quebec, Laval, Quebec, Canada). GFP-Rab-14, GFP-Rab-21 and their mutants were from Dr. James Cardelli (Louisiana State University, Shreveport, LA). GFP-Rab15 and mutants were from Dr. Lisa Elferink (University of Texas Medical Branch, Galveston, TX). GFP-Rab11a and GFP-Rab11b were from Dr. James Goldenring (Medical College of Georgia, Augusta, GA). Canine Rab22a and mutants were from Dr. V. Olkkonen (National Public Health Institute, Helsinki, Finland) and were subcloned into the *Bam*HI site of either the pEGFP-C1 vector (BD Biosciences Clontech, Palo Alto, CA) or the pFLAG-cmv6 (Sigma-Aldrich), placing the GFP and FLAG tags on the N terminus of the protein. Arf6 and mutants are in pXS plasmid (Radhakrishna and Donaldson, 1997). For transfection, cells were plated and transfected the next day using FuGene (Roche Diagnostics, Indianapolis, IN). Experiments were performed 16–20 h after transfection.

Polyclonal Antibody against Rab22a

The carboxy terminus of human Rab22a differs from the carboxy terminus of other members of the Rab family. A peptide corresponding to a stretch of 16 amino acids located at the carboxy terminus of the human Rab22a (residue170–185, DANLPSGGKGFKLRRQ) was conjugated to KLH via a cysteine residue added to the amino-terminal end of the peptide. Rabbits were immunized with the conjugate, and the serum was collected and tested for Rab22a immunoactivity and compared with preimmune serum collected before immunization (Zymed Laboratories).

Electrophoresis and Immunoblotting

HeLa cells were grown on 15-cm petri dishes. After the appropriate treatment (transfection, siRNA treatment, etc.), cells were washed three times in cold phosphate-buffered saline (PBS), harvested by using a tissue culture cell scraper, and pelleted by centrifugation at 4°C (1200 × *g* for 10 min). Pellets were solubilized in sample buffer, and samples containing 15–20 μg of protein were separated by 10–20% SDS-PAGE, transferred to nitrocellulose paper, and probed with the appropriate antibody.

Immunofluorescence, Confocal Analysis, and Time-Lapse Imaging

Cells were plated on glass coverslips and transfected the next day. For uptake of Tfn, untransfected cells were serum starved for 30 min at 37°C in DMEM containing 0.5% bovine serum albumin, and then 5 μg/ml fluorescently labeled Tfn was added. Internalization of MHCI monoclonal antibody (W6/32) was performed as described previously (Brown *et al*., 2001). Cells were fixed with 2% formaldehyde/PBS at room temperature for 10 min and stained in blocking solution (PBS containing 10% fetal calf serum and 0.2% saponin). The internalized antibodies were visualized with the appropriate secondary antibodies. All images were obtained using a 510 LSM confocal microscope (Carl Zeiss, Thornwood, NJ) with 63× Plan Apo objective as described previously (Naslavsky *et al*., 2003). Acquisition of figures was accomplished in Adobe Photoshop 5.5. Live cell images were acquired every 6 s, at 37°C, by using CO_2-independent media (Invitrogen, Carlsbad, CA). Videos were generated using MetaMorph (Universal Imaging, Downingtown, PA).

Scoring of MHCI-containing Tubules and Peripheral Vesicles

After the internalization of MHCI, cells were fixed and processed for immunofluorescence as described above. Sample were analyzed with an epifluorescence photomicroscope (Carl Zeiss) with a 63×/1.4 Plan Apo chromate objective. Transfected cells were first identified on the 488 channel and then analyzed switching to the 594 channel. Fifty to 100 cells per coverslip (two coverslips per condition) were scored for the presence of MHCI-containing tubular structures and MHCI-containing peripheral vesicles. The percentage of cells having either tubules or peripheral vesicles was calculated and expressed as percentage of the nontransfected cells (control). Data are averages of two or three independent experiments ± SEM.

Recycling Assay for MHCI and Transferrin

To measure MHCI recycling to the plasma membrane, HeLa cells were grown on glass coverslips and incubated on ice for 30 min with the W6/32 antibody directed against MHCI. Cells were then washed with ice-cold medium to remove the unbound antibody and incubated at 37°C in the presence of 1 μM LatA. At the end of the internalization, the antibody that was not internalized was removed by stripping with a low pH buffer (0.5% acetic acid, 0.5 M NaCl, pH 3.0). Cells were washed twice in PBS and twice in DMEM, and then incubated at 37°C for 30 min (unless otherwise specified) with complete medium to allow the recycling of MHCI. A set of cells were processed immediately after the washing steps (time 0). To reveal the surface pool of MHCI, a set of coverslips were fixed at the end of the incubation and incubated with a 594-Alexa–conjugated antibody directed against mouse IgG (594-GAM). To reveal the internal pool of MHCI, another set of coverslip were treated again with the low pH buffer, fixed, and incubated with a 594-GAM in the presence of 0.2% saponin. The amount of MHCI at the surface or inside the cell was estimated as follows: 30–50 cells/coverslip were randomly selected and imaged using a 510 LSM confocal microscope (Carl Zeiss) with a 40× plan Apo objective. The pinhole was completely open, and all the images were taken with identical acquisition parameters, those previously optimized for the fluorescent signals to be in the dynamic range. Under these conditions, the amount of MHCI is proportional to the total fluorescence. For each channel the total fluorescence of each individual cell was measured using LSM image examiner (version 3.01; Carl Zeiss). "Recycled MHCI" was calculated by expressing the surface MHCI as a percentage of the total MHCI (sum of the internal and the surface MHCI) with background subtracted (recycled MHCI at time 0).

To measure the recycling of Tfn, cells were serum starved for 30 min at 37°C in DMEM containing 0.5% bovine serum albumin and 5 μg/ml Alexa 595-Tfn (594-Tfn) were internalized for 30 min. At the end of the internalization, cells were stripped of the noninternalized Tfn as described above and incubated in complete medium for different times. Cells were fixed, and the amount of 594-Tfn inside the cell was estimated as described for MHCI and expressed as percentage of the Tfn at time 0. Recycled Tfn at a given time was calculated as the difference between the percentage of Tfn at time 0 (100%) and the percentage of internal Tfn left at a given time.

siRNA Depletion

HeLa cells were seeded on a 10-cm dish and grown in complete medium without antibiotics. The first treatment was performed after 24 h. For each dish, 24 μl of Oligofectamine were added to 66 μl of Opti-MEM (Invitrogen),

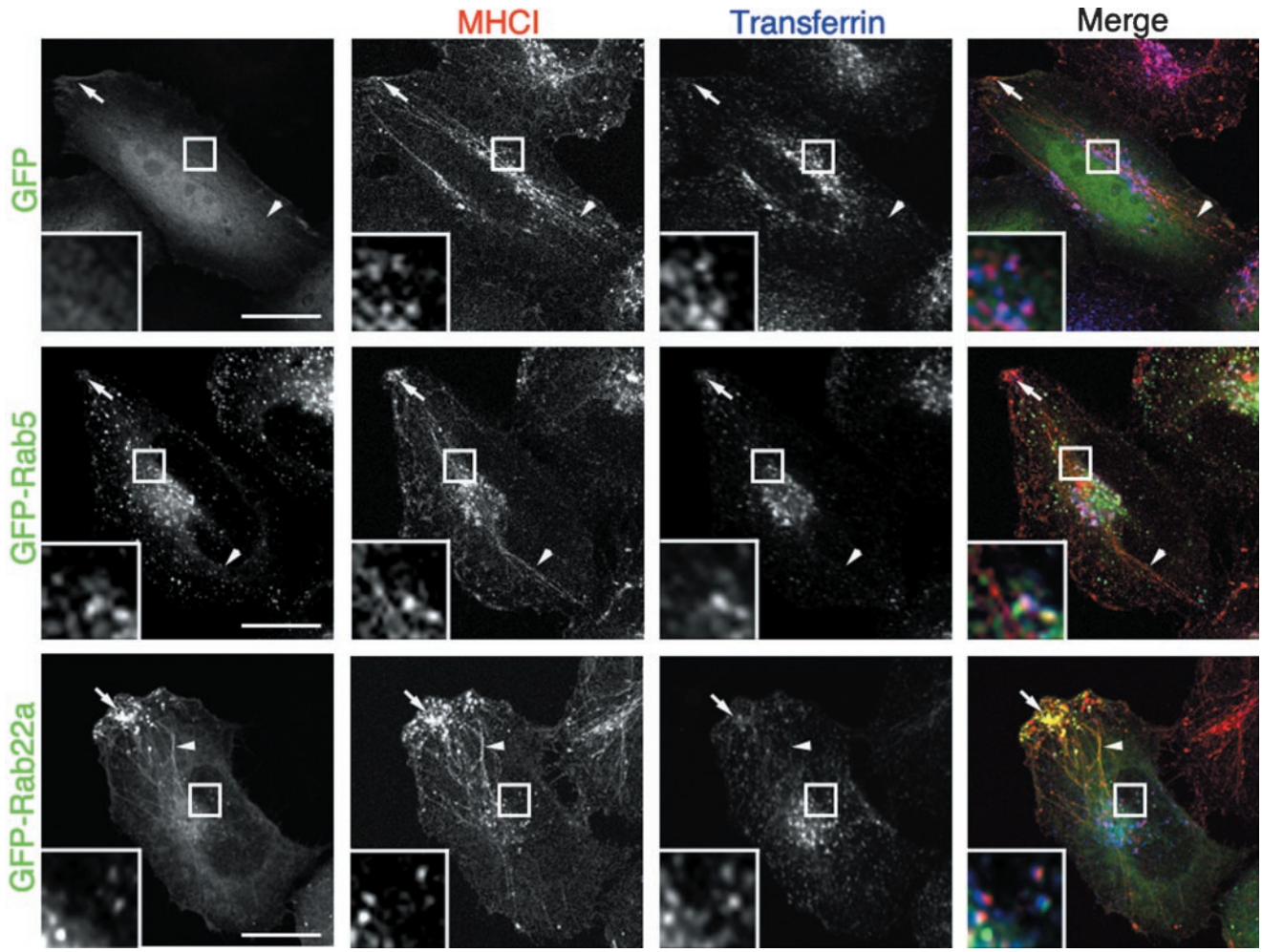

Figure 1. MHCI colocalizes with GFP-Rab22a on tubular endosomes. HeLa cells were transiently transfected with either GFP (top), GFP-Rab5 (middle), or GFP-Rab22a (bottom) for 20 h and then incubated for 30 min at 37°C in the presence of an antibody against MHCI and 633-Tfn and processed for confocal microscopy as described in MATERIALS AND METHODS. Arrowheads point to MHCI-containing tubules, and arrows point to MHCI-containing peripheral vesicles. Insets show a magnification of the juxtanuclear area where MHCI endosomes also contain Tfn (merge compartment). Bar, 10 μm.

and the solution was incubated for 5–10 min at room temperature. This was mixed with a second solution containing 970 μl of Opti-MEM plus 300 pmol of siRNA. The mixture was incubated at room temperature for 15–20 min and added to the cells. After 72 h, the cells were trypsinized, diluted 1:10, and seeded in a 10-cm dish with or without coverslips. Then, after 6 h, the second treatment with siRNA was performed, and cells were used after an additional 72 h. The target sequence for the human Rab22a (AAGGACUACGCCGACUCUAUU) was designed using the QIAGEN software available at http://www1.qiagen.com/siRNA/ and was synthesized as Option C siRNA by Dharmacon (Lafayette, CO).

RESULTS

Rab22a Localizes on Nonclathrin-derived Endosomes

We examined whether any of the Rab proteins known to have a role in endosomal trafficking colocalized with the nonclathrin-derived endosomal pathway. Due to the lack of good immunological reagents suited to detect endogenous Rab proteins, we transiently transfected HeLa cells with various GFP-tagged Rabs (Rab4, Rab5, Rab7, Rab11a, Rab11b, Rab14, Rab15, Rab21, Rab22a, and Rab25) because, in most instances, the GFP tag does not affect either the localization or the function of the Rab proteins (Sonnichsen *et al*., 2000). To label the clathrin-independent and the clathrin-dependent endosomal systems, respectively, Rab-transfected cells were allowed to internalize an antibody directed against MHCI and Alexa-633–conjugated Tfn (633-Tfn) for 30 min. In control cells (either untransfected or transfected with the empty GFP vector), MHCI was localized 1) in vesicular endosomes located in the perinuclear area that contained Tfn (Figure 1, top, inset), hereafter referred to as the merge compartment (Naslavsky *et al*., 2003); 2) in tubular recycling endosomes devoid of Tfn emanating from the perinuclear area and occasionally observed originating from endosomal structures which contained Tfn (Figure 1, top, arrowheads); and 3) in vesicular structures clustered at the cell periphery and devoid of Tfn (Figure 1, top, arrows). In 40–60% of the cells, the tubular endosomes extended for several micrometers from the juxtanuclear region, whereas in the other cells tubules were much shorter (our unpublished observations). These long tubular structures were not an artifact of fixation or specimen processing because they also could be visualized by time-lapse imaging of living cells (see below). The reason why long tubules were not seen in all cells is not clear.

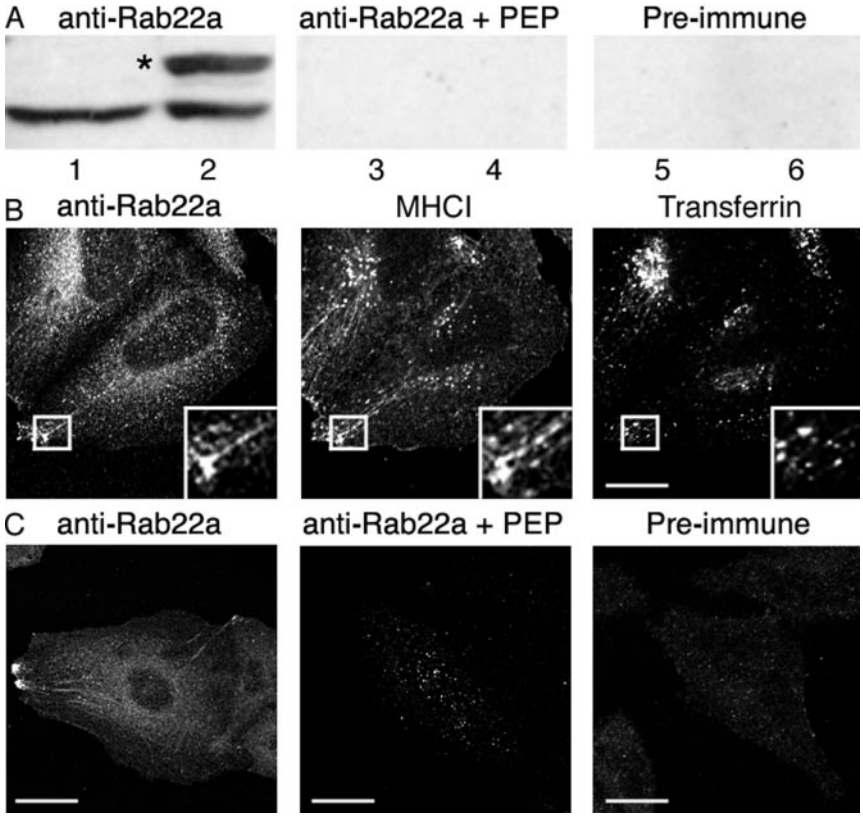

Figure 2. Detection of endogenous Rab22a with a specific antibody. (A) Lysates from nontransfected (lanes 1, 3, and 5) and FLAG-Rab22a-transfected (lanes 2, 4, and 6) HeLa cells were probed with a Rab22a-antiserum in the absence (lanes 1 and 2) or in the presence (lanes 3 and 4) of the peptide against which the antiserum was raised, or with the preimmune serum (lanes 5 and 6). The asterisk denotes the position of the FLAG-tagged Rab22a protein. (B) Nontransfected HeLa cells were fixed and stained with either the Rab22a antiserum in the presence or the absence of the peptide against which the antiserum was raised, or with a preimmune serum. Bar, 10 μm. (C) Nontransfected HeLa cells were incubated with antibody against MHCI and 633-Tfn for 30 min as described in Figure 1, and after fixation, probed with the Rab22a-antiserum followed by the Alexa-488 goat anti-rabbit IgG.

When overexpressed at a low level, most of the Rabs did not affect the morphology of either the clathrin-independent or the clathrin-dependent pathway. Rab5 (Figure 1, middle) and to a minor extent Rab4, Rab14, and Rab21 (our unpublished observations) were localized on the merge compartment (Figure 1, middle, inset), but were not present on the MHCI-containing endosomes devoid of Tfn (tubules and peripheral vesicles; Figure 1, middle, arrows and arrowheads). Rab7, Rab15, and Rab25 did not colocalize with MHCI under these experimental conditions (our unpublished observations). Rab11a and Rab11b occasionally localized to the MHCI-containing tubular endosomes and only partially overlapped with the merge compartment (our unpublished observations). Strikingly, Rab22a showed a distinct, overlapping pattern. At low level of expression Rab22a colocalized with MHCI in the tubules and in the peripheral vesicles that were both devoid of Tfn (Figure 1, bottom, arrows and arrowheads) and occasionally localized with MHCI and Tfn in the merge compartment (Figure 1, bottom, inset). Similar results were obtained overexpressing Rab22a in other cell types (e.g., Cos7 and A431; our unpublished data) or overexpressing Rab22a tagged with either a myc or a FLAG tag (our unpublished observations).

Next, we examined whether endogenous Rab22a also localized on the nonclathrin-derived endosomes and to this aim, we generated a polyclonal antibody directed against the carboxy terminus of human Rab22a (see MATERIALS AND METHODS). The Rab22a antiserum was first tested by immunoblotting lysates from either FLAG-Rab22a–transfected or nontransfected HeLa cells. In untransfected cells, the antiserum recognized a single band of the predicted molecular size for Rab22a (Figure 2A, lane 1). The band was not detected by Rab22a antiserum that was preincubated with the immunizing peptide (Figure 2A, lane 3) or by preimmune serum (Figure 2A, lane 5). The Rab22a antibody detected the overexpressed protein, which ran at a slightly higher molecular weight due to the FLAG tag (Figure 2A, lane 2, asterisk), but did not recognize any of the other Rabs overexpressed as controls (our unpublished observations). Similar results were obtained with lysates derived from other cell types and tissues (Cos7, A431, and bovine brain; our unpublished observations).

Next, we examined whether the Rab22a antibody could specifically label Rab22a in cells. Importantly, the Rab22 antiserum detected the overexpressed Rab22a, but did not recognize any of the other Rab proteins that were overexpressed as controls (our unpublished observations). Nontransfected HeLa cells that had internalized MHCI and 633-Tfn for 30 min were probed with the Rab22a antiserum. The endogenous Rab22a localized on both the tubular endosomes and the vesicles at the cell periphery, which contained MHCI but did not contain Tfn (Figure 2B, inset), and only occasionally did we observe labeling of the merge compartment. The labeling of the endosomal structures was neither detected by preimmune serum nor by the Rab22a antiserum that was preincubated with the immunizing peptide (Figure 2C).

Because Rab11a and Rab11b also were occasionally localized on the MHCI-containing tubules, we checked whether the endogenous Rab11 also was present on these structures. MHCI-containing tubules but not other MHCI-containing endosomes were indeed occasionally labeled by an affinity-purified antibody directed against Rab11a (Volpicelli *et al.*, 2002). However, the extent and frequency of the labeling was much lower than by Rab22a antibody (our unpublished observations).

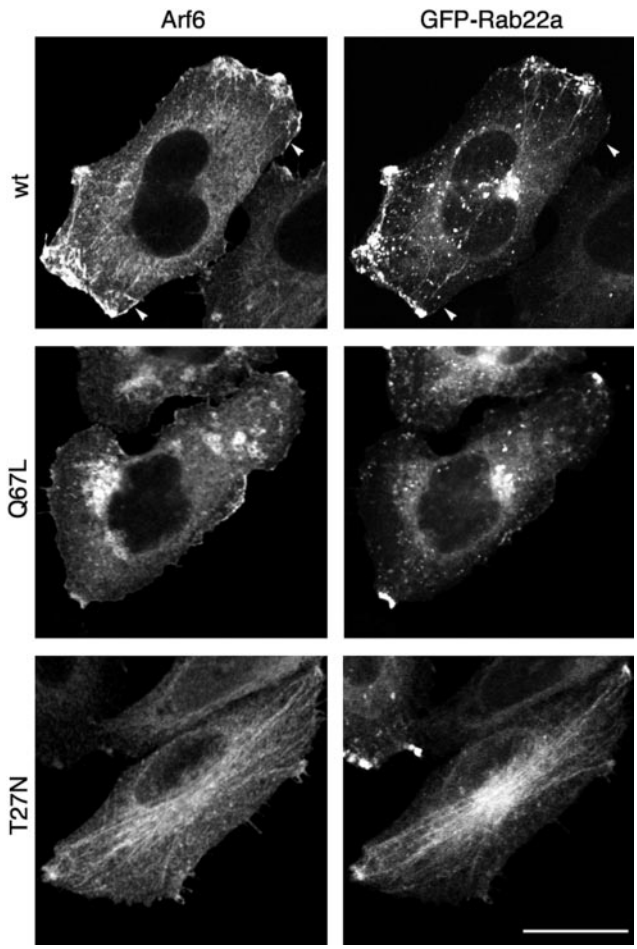

Figure 3. GFP-Rab22a is not localized on the vacuoles accumulated in Arf6-Q67L–expressing cells. HeLa cells were cotransfected with GFP-Rab22a and either Arf6-wt (top), Arf6-Q67L (middle), or Arf6-T27N (bottom). Cells were probed with a polyclonal antiserum directed against Arf6 followed by the Alexa-594-goat anti rabbit IgG. Arrowheads point to region of the PM where Arf6 does not colocalize with GFP-Rab22a. Bar, 10 μm.

Rab22a Is Associated with the Recycling Endosome and Not the Incoming Clathrin-independent Endosome

The tubular endosomes containing MHCI also have Arf6 associated with them and have been implicated in the recycling of MHCI back to the PM (Radhakrishna and Donaldson, 1997; Caplan *et al*., 2002; Naslavsky *et al*., 2003). Because Arf6 is associated with both the incoming and outgoing transport carriers of this clathrin-independent endosomal system, we examined where Rab22a was localized with respect to Arf6 and its mutants. We used expression of GFP-Rab22a to visualize Rab22a because it localized similarly to endogenous Rab22a with the exception that GFP-Rab22a also localized to the merge compartment (see DISCUSSION). Additionally, GFP-Rab22 had the advantages of a strong fluorescent signal and better resolution. In cells expressing wild-type Arf6, GFP-Rab22a colocalized with Arf6 on the tubular endosomal membranes and on peripheral vesicles that accumulated at the periphery of the cells (Figure 3, top), but it did not colocalize with Arf6 on the PM, where Arf6 is believed to be in its active, GTP-bound form (Figure 3, top, arrowheads). Expression of the constitutively active mutant of Arf6 (Arf6-Q67L) blocks the clathrin-independent endosomal pathway shortly after internalization; it causes the Arf6 early endosomal structures to undergo fusion, leading to the accumulation of large vacuolar structures, enriched in phosphatidylinositol bisphosphate and actin, that trap Arf6 and cargo molecules (Brown *et al*., 2001; Naslavsky *et al*., 2003). Under these conditions, both the convergence of the nonclathrin-derived endosomes with the early endosomes and the recycling to the plasma membrane are inhibited (Naslavsky *et al*., 2003; our unpublished data). Remarkably, GFP-Rab22a did not associate with the vacuoles formed in cells expressing Arf6-Q67L (Figure 3, middle). Furthermore, GFP-Rab22a–labeled tubules were no longer observed and the number of Rab22a-labeled peripheral vesicles was significantly decreased. Conversely, in cells expressing the inactive, dominant negative mutant of Arf6 (Arf6-T27N), GFP-Rab22a was localized predominantly on the Arf6-labeled tubules, and fewer peripheral vesicles also were observed (Figure 3, bottom). In all of the cells, the prominent juxtanuclear distribution of GFP-Rab22a represents the merge compartment that also contained the transferrin receptor (our unpublished observations), and as mentioned above, this localization is not observed for the endogenous protein. Endogenous Rab22a localized on the Arf6-labeled tubules in both Arf6 wt- and Arf6 T27N-expressing cells, whereas it was not localized onto the vacuoles in Arf6-Q67L–expressing cells (our unpublished observations). These data suggest that Rab22a is not associated with Arf6 at the PM or on early endosomal structures, but rather on the outgoing recycling arm of the pathway.

To confirm that Rab22a is associated with MHCI on outgoing recycling structures and not on incoming early endosomes, we compared internalization at early and late times. MHCI and 633-Tfn were internalized for 5 min in HeLa cells that were transiently transfected with GFP-Rab22a. As described previously, after 5 min of uptake, MHCI and Tfn were found on distinct endosomes, mostly vesicular in nature (Naslavsky *et al*., 2003) that were not labeled by GFP-Rab22a (Figure 4A, inset). Tubules and peripheral vesicles that were labeled with GFP-Rab22a were mostly devoid of both MHCI and Tfn (Figure 4A, arrowheads). A similar experiment was performed using time-lapse imaging. Movie-1 (see Supplementary Information) and Figure 4B show a cell transfected with GFP-Rab22a after the addition of an antibody against MHCI that was conjugated to Cy3 (Cy3-MHCI). At early time points, MHCI-containing endosomes occurred close to the PM and at the bottom of the cell (Figure 4B, 1′ and inset). These pleiomorphic structures were not labeled with GFP-Rab22a, and none of the GFP-Rab22a-labeled tubules and vesicles contained any MHCI. After 5 min, some Rab22a-labeled tubules seemed to contain MHCI and also some vesicular structures in the perinuclear area (Figure 4B, 5′, 10′, and 20′, and insets). The amount of MHCI in GFP-Rab22a tubules increased over time. The overexpression of GFP-Rab22a did not alter either the kinetics of internalization or the morphology of the MHCI tubules compared with the adjacent nontransfected cell. In Movie 2 (see Supplementary Information), the movement of GFP-Rab22a–labeled tubules from the perinuclear area to the cell periphery is shown along with the disappearance of the tubules in the cluster of peripheral vesicles. In some cases, tubules are seen breaking down into small vesicles before fusion.

Together, these data suggest that Rab22a associates with the nonclathrin-derived cargo at a later stage of the endocytic processes, after the convergence of nonclathrin derived endosomes with the early endosomes, and during recycling.

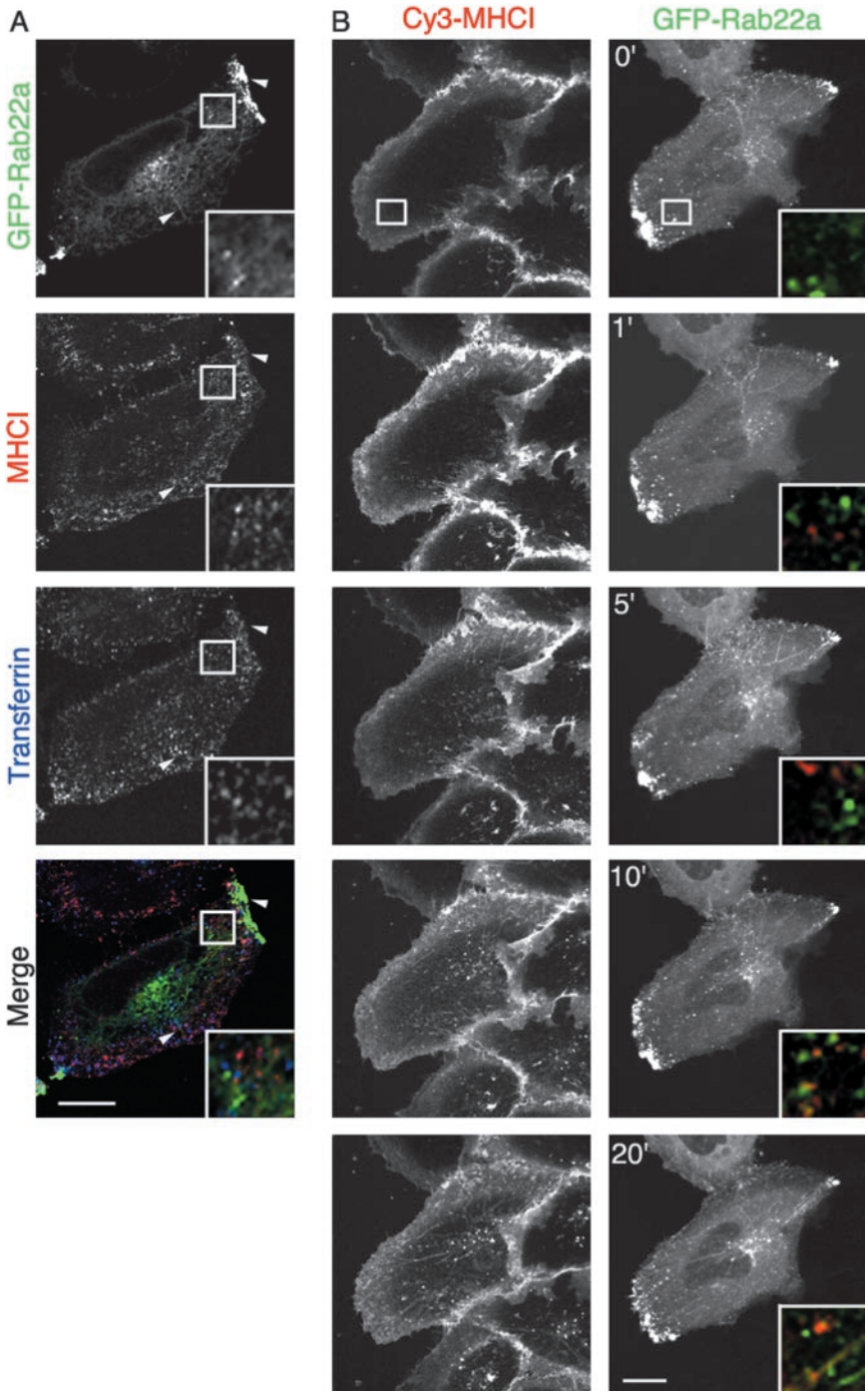

Figure 4. Rab22a is associated with the recycling endosomes and not with the incoming, nonclathrin-derived endosomes. (A) HeLa cells overexpressing GFP-Rab22a were allowed to internalize an antibody against MHCI and 633-Tfn for 5 min. Cells were fixed and processed for confocal microscopy as described in MATERIALS AND METHODS. Arrowheads point to tubules and peripheral vesicles that are labeled with GFP-Rab22a but do not contain either MHCI or Tfn. Inset shows that MHCI- and Tfn-containing endosomes are not labeled with GFP-Rab22a. (B) HeLa cells were transfected with GFP-Rab22a, and after 24 h cy3-conjugated MHCI was added to the medium (time 0′). Cells were immediately imaged as described in MATERIALS AND METHODS (movie available as Supplementary Information), and images acquired at different times are shown in this figure. Insets show the color-merged colocalization of cy3-MHCI and GFP-Rab22a at different times from the same area indicated by the box in the top panel. Bars, 10 μm.

Expression of Rab22a-S19N Inhibits the Formation of Tubular Recycling Endosomes Containing MHCI

Because Rab22a is localized on the recycling endosomes, we wondered whether its activity might regulate recycling. To address this question, we used two mutants of Rab22a that are impaired in the GTP cycle: Rab22a-Q64L, defective in GTP hydrolysis, and Rab22a-S19N, defective in GTP binding (Mesa *et al.*, 2001; Kauppi *et al.*, 2002). HeLa cells were transiently transfected with either GFP-Rab22a-Q64L or GFP-Rab22a-S19N and allowed to internalize MHCI antibody and 633-Tfn for 30 min. Rab22a-Q64L localized to tubular structures and peripheral vesicles that contained MHCI but not Tfn (Figure 5A). The phenotype was almost identical to that of the wild-type protein, although larger MHCI-containing structures could be observed at the periphery, and the number of cells showing MHCI- and Rab22a-positive tubules was significantly increased (Figure 5B).

Strikingly, in cell expressing Rab22a-S19N, tubular structures and vesicles at the cell periphery were no longer observed (Figure 5, A and B), and MHCI and Tfn were clustered in the perinuclear area in a compartment (Figure 5A, arrowheads) that was labeled by an antibody against Rab11a but not by an antibody against Rab4 (our unpublished observations). Rab22a-S19N was localized to the cytoplasm

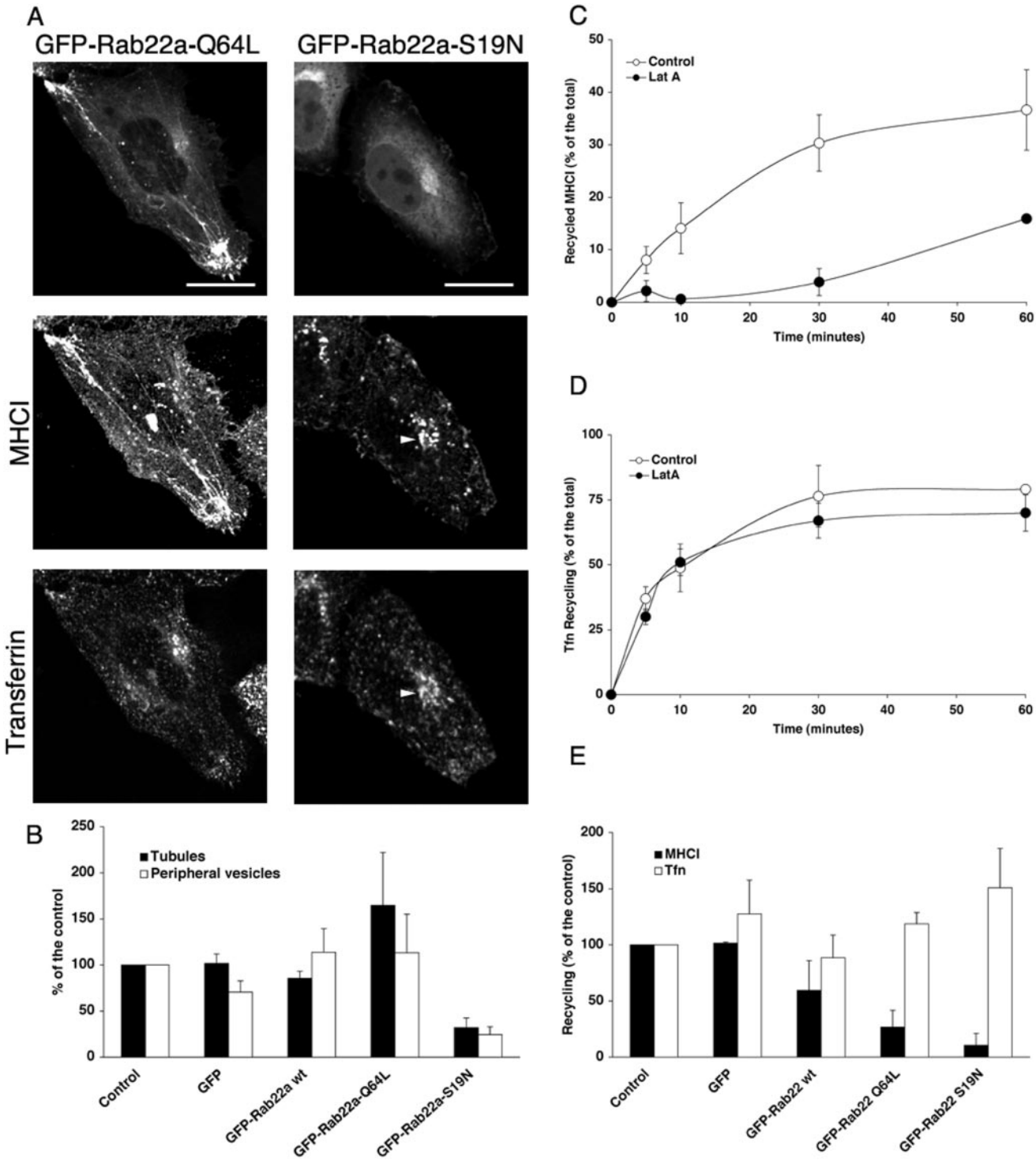

Figure 5. Expression of Rab22a mutants alters the morphology of the MHCI-containing endosomes and inhibits recycling of MHCI, but not of Tfn, back to the plasma membrane. (A) HeLa cells transfected with either GFP-Rab22a-Q64L or GFP-Rab22a-S19N were loaded with antibody to MHCI and 633-Tfn and processed as described in Figure 1. Bars, 10 μm. (B) HeLa cells were transfected as indicated, loaded with antibody to MHCI as described in legend to Figure 1, and scored as described in MATERIALS AND METHODS for the presence of MHCI-containing tubules (closed bars) or MHCI-containing peripheral vesicles (open bars). Data are averages of three independent experiments ± SEM. (C) HeLa cells were allowed to internalize MHCI in the presence of LatA for 30 min at 37°C. At the end of the internalization, the surface MHCI was stripped by mild acid washing, and cells were then incubated for different times with complete medium in the absence (open circles) or in the presence of 1 μM LatA (closed circles). Recycling was estimated as described in MATERIALS AND METHODS. Data are averages of two independent experiments ± SEM. (D) HeLa cells were allowed to internalize 594-Tfn for 30 min. At the end of the internalization, surface Tfn was stripped and cells were incubated for different times at 37°C in complete medium in the absence (open circles) or in the presence of 1 μM LatA (closed circles). Recycling was estimated as described in MATERIALS AND METHODS. Data are averages of two independent experiments ± SEM. (E) HeLa cells either nontransfected (control) or transfected as

and to a structure in the perinuclear area (Figure 5A) that colocalized with GM130, a marker for the Golgi apparatus (our unpublished observations and previously reported by Kauppi *et al*., 2002). At low levels of expression of either the wild type or mutants of Rab22a, we did not observe any effect on Golgi morphology (our unpublished observations). However, the Golgi became fragmented upon high expression of wild-type or Q64L mutant of Rab22a (our unpublished observations) as had been observed previously (Kauppi *et al*., 2002).

Expression of Rab22a and Its Mutants Inhibits the Recycling of MHCI but Not Tfn to the PM

Because Rab22a is localized on MHCI tubules that were suggested to mediate the recycling of MHCI to the PM (Radhakrishna and Donaldson, 1997; Caplan *et al*., 2002) and the overexpression of GFP-Rab22a-S19N significantly reduced the number of tubules in HeLa cells, we examined whether Rab22a was required for recycling of MHCI back to the PM. Recycling of MHCI was estimated by measuring the amount of MHCI reappearing at the PM after its accumulation in the recycling compartment (Radhakrishna and Donaldson, 1997; see MATERIALS AND METHODS). We previously showed that treatment of cells with cytochalasin D, an inhibitor of actin polymerization, reversibly inhibits MHCI recycling causing MHCI to accumulate in the tubular endosomes (Radhakrishna and Donaldson, 1997). In these experiments, we used LatA, another actin inhibitor, to accumulate MHCI in the tubular endosomes because LatA was less toxic to the cell. Figure 5C (white circles) shows the time course of the reappearance of MHCI to the surface with the maximal amount of recycling occurring at ≈30 min. Strikingly, the continuous presence of LatA in the medium significantly inhibited recycling of MHCI (Figure 5C, black circles), whereas it had no effect on the recycling of Tfn (Figure 5D).

To study the effect of Rab22a and its mutants on the recycling of MHCI, HeLa cells were transiently transfected with GFP-Rab22a wt, GFP-Rab22a-Q64L, or GFP-Rab22a-S19N, and the amount of recycled MHCI was estimated as described above. Expression of the dominant negative mutant of Rab22a, S19N, resulted in a significant inhibition in recycling of MHCI compared with nontransfected or GFP-transfected controls (Figure 5E, solid bars). Expression of the constitutively active mutant Q64L also inhibited recycling as potently as S19N mutant (Figure 5E, solid bars), suggesting that both activation and inactivation of Rab22a was required for recycling of MHCI. Some inhibition of MHCI recycling also was observed in cells expressing wild-type Rab22a (Figure 5E, solid bars). Notably, neither Rab22a nor its mutants affected the recycling of Tfn to the PM (Figure 5E, open bars), as had been reported previously (Kauppi *et al*., 2002).

Figure 5 (cont). indicated were allowed to internalize and recycle MHCI (closed bars) or Tfn (open bars) as described in MATERIALS AND METHODS. Recycling of MHCI was measured after 30 min from the release of the LatA block, whereas Tfn recycling was measured after 10 min from the incubation in complete medium. Data, normalized for the control, are averages of either three (MHCI) or two (Tfn) independent experiments ± SEM. One-way analysis of variance was used to test the statistical significance of the data. For MHCI recycling, the p values for the Tukey's honestly significant difference test were control/GFP versus Rab22aWT, $p < 0.05$; control/GFP versus Rab22Q64L, $p < 0.01$; and control/GFP versus Rab22aS19N, $p < 0.01$. For transferrin recycling, p values were not significant.

Rab22a seems to specifically regulate the recycling of MHCI to the plasma membrane. The inhibition of recycling caused by overexpression of Rab22a and its mutants was not due to an effect on the internalization of MHCI (our unpublished observations) or an inhibition of fusion between MHCI-containing and clathrin-derived endosomes. We did not observe any qualitative (Figure 5A) or quantitative (our unpublished observations) difference in the fusion between the MHCI-containing and the transferrin-containing endosomes. The lack of effect of Rab22a constructs on the internalization of both MHCI and Tfn (our unpublished observations) is consistent with the fact that neither the endogenous nor the overexpressed Rab22a were localized on the incoming endosomes at early times of internalization (Figures 3 and 4 and Movie 1).

siRNA-mediated Depletion of Rab22a Delays MHCI Recycling to the PM

Overexpression of Rab22a and its mutants affects recycling of MHCI. Surprisingly, both the "active" (wt and Q64L) and the "inactive" (S19N) forms of Rab22a impaired recycling. The impairment could be due to the perturbation of the GTP cycle of Rab22a, cellular levels of Rab22a, or to the sequestration of some GEF or GAP that Rab22a might have in common with other Rab proteins. To determine whether endogenous Rab22a regulates recycling, HeLa cells were treated with a siRNA directed against Rab22a to reduce the endogenous levels of Rab22a, as described in MATERIALS AND METHODS. The efficiency of Rab22a depletion was first assessed by immunoblotting. In siRNA-treated cells, Rab22a was depleted below the detection level, whereas other proteins (namely, Rab4, Rab5, Rab11, Arf6, TfnR, and actin) were not affected (Figure 6A). The siRNA-treated cells had normal morphology and could be grown for several passages in the presence of the siRNA. In siRNA-treated cells, labeling with the Rab22a-antiserum was greatly diminished (Figure 6B) and when Rab22a-depleted cells were allowed to internalize cy3-MHCI and 633-Tfn, the percentage of cells showing MHCI-containing tubular structures and peripheral vesicles was significantly reduced, as previously seen when Rab22a-S19N was expressed (compare Figures 5B and 6C). The trafficking of Tfn was not impaired, and the morphology of other organelles in both the secretory (Golgi and endoplasmic reticulum) and the endocytic pathway (early endosomes and lysosomes) was not affected (our unpublished observations). Recycling of MHCI back to the PM also was measured in siRNA-treated cells. The recycling of MHCI to the PM was substantially inhibited, whereas the recycling of Tfn was slightly inhibited (Figure 6D). The internalization of MHCI and Tfn was not altered in siRNA-treated cells (our unpublished observations).

Expression of Rab11a-S25N Inhibits Recycling of MHCI to the Plasma Membrane

Rab11 has been implicated in the recycling of membranes from the juxtanuclear endocytic recycling compartment (ERC) (Ullrich *et al*., 1996; Volpicelli *et al*., 2002), and recently a dominant negative mutant of Rab11a has been shown to inhibit the recycling to the plasma membrane of Integrin $\beta 1$ (Powelka *et al*., 2004), a molecule known to traffic with MHCI (Radhakrishna and Donaldson, 1997). Because both exogenous Rab11a and endogenous Rab11a were localized on the tubules (our unpublished observations), we investigated whether Rab11a and Rab22a regulate the same steps in the recycling of MHCI to the PM. HeLa cells overexpressing the dominant negative mutant of Rab11a (GFP-Rab11a-S25N) were allowed to internalize antibody to MHCI and

633-Tfn for 30 min. In cells expressing GFP-Rab11a-S25N, internalized MHCI was localized in tubular structures and in the perinuclear area, but it was no longer present in peripheral vesicles in cells (Figure 7A). Fusion of MHCI-containing endosomes with Tfn-containing endosomes was not affected (our unpublished observations). Strikingly, expression of GFP-Rab11a-S25N did not affect the percentage of cell showing MHCI-containing tubules, whereas the percentage of cells showing MHCI in peripheral vesicles was reduced (Figure 7B). The overexpression of GFP-Rab11a-S25N impaired the recycling of both MHCI and Tfn (Figure 7C) as reported previously (Ullrich *et al*., 1996; Schlierf *et al*., 2000; Powelka *et al*., 2004). GFP-Rab11a-S25N localized to the juxtanuclear region and partially overlapped with TfnR and Golgi markers, but no alteration in Golgi structure was observed (our unpublished observations). Expression of the dominant negative mutant of Rab11b (GFP-Rab11b-S25N), a related isoform of Rab11a, gave similar results (our unpublished observations).

DISCUSSION

Endogenous Rab22a Is Localized on MHCI-containing Recycling Endosomes

In this study, we show that Rab22a associates with and regulates the formation of recycling endosomal structures that return proteins internalized independently of clathrin back to the PM. Using both overexpression of GFP-Rab22a and localization of endogenous Rab22a with a Rab22a-specific antiserum, we show that Rab22a is associated with tubular endosomes and vesicles located at the cell periphery. These tubular and vesicular structures contain cargo (e.g., MHCI) that enter cells in nonclathrin vesicles (NV) and lack cargo (e.g., Tfn receptor) that enter cells in clathrin vesicles (Figure 8). When overexpressed, Rab22a also localized with the "merge" compartment containing Tfn and its receptor, as reported previously by others (Mesa *et al*., 2001; Kauppi *et al*., 2002). However, we did not observe this localization for endogenous Rab22a. This suggests that endogenous Rab22a either is not present or is present at very low levels and/or transiently on the merge compartment. Given the juxtanuclear location, it seems likely that this merge compartment from which Rab22a tubules emerge is the endocytic recycling compartment or ERC.

Several lines of evidence support the conclusion that the tubular endosomes that are labeled with the antibody against Rab22a are outgoing, recycling endosomes. First, the expression of mutants of Arf6, the constitutively active Q67L and GTP-binding defective T27N, block the clathrin-independent endosomal pathway. Cells expressing Arf6-Q67L accumulate MHCI in early Arf6 endosomal structures, blocking both convergence with clathrin cargo in the early endosome (EE) and recycling back to the PM (Brown *et al*., 2001; Naslavsky *et al*., 2003). Neither endogenous nor overexpressed Rab22a localized with these accumulating endosomes. By contrast, endogenous Rab22a and also overexpressed Rab22a colocalized with Arf6-T27N on tubular recycling endosomes that accumulate in cells expressing this mutant (Radhakrishna and Donaldson, 1997). Second, newly internalized MHCI does not reach Rab22a-containing compartments until 5–10 min after internalization (Figure 4), a time that coincides with the appearance of MHCI in tubular endosomes and recycling back to the PM (Caplan *et al*., 2002). As shown using time-lapse imaging, MHCI is internalized in small pleiomorphic structures that do not contain Rab22a (Figure 4 and Movie 1) and later occurs in the Rab22a-associated tubules and in the cluster of vesicles accumulated at the cell periphery.

Two previous studies using transfection of Rab22a reported that Rab22a had a unique distribution on endosomal membranes and that expression of the wild-type and mutant forms of Rab22a affected endosomal morphology and trafficking (Mesa *et al*., 2001; Kauppi *et al*., 2002). Overexpressed Rab22a was found on enlarged early endosomes that also labeled with EEA1 (Kauppi *et al*., 2002), and some tubular membrane labeling also was observed (Mesa *et al*., 2001). The localization to early and late endosomes in these studies could be due to the high level of expression of Rab22a because we also observed enlarged structures that colocalized with EEA1 in cells expressing high levels of Rab22a (our unpublished observations). Our studies suggest a more limited distribution of Rab22a because we are able to localize the endogenous protein. A tubular localization for Rab22b/31, a closely related protein, was observed in an earlier study where it was suggested to mediate Golgi to PM transport, although colocalization with secretory proteins was unpublished observations in that study (Rodriguez-Gabin *et al*., 2001). Based on this tubular localization, it is possible that Rab22b would localize and function similar to what we observed with Rab22a.

Rab22a Specifically Regulates the Recycling of MHCI to the PM

Because Rab22a had been found to bind to EEA1 (Kauppi *et al*., 2002), we had thought that Rab22a could function to regulate fusion of the NV with the early endosome. Although it is still possible that the interaction with EEA1 may play a role in Rab22a function, the localization of endogenous Rab22a revealed that it was associated with the outgoing, recycling arm of the pathway. To probe the specific function of Rab22a in recycling, we overexpressed wild-type, constitutively active (Rab22a-Q64L), and inactive (Rab22a-S19N) mutants of Rab22a and also examined the effect of reduced expression of endogenous Rab22a by siRNA. Loss of Rab22a function, either by expression of Rab22a-S19N or siRNA, inhibited the recycling of MHCI back to the PM (Figures 5 and 6), whereas having only a minor effect on TfnR recycling. Lack of Rab22a function also resulted in a dramatic loss of tubular endosomes containing MHCI (Figures 5 and 6) and of the peripheral vesicle accumulations that occur at the edges of cells (Figures 5 and 6). These observations provide compelling evidence that Rab22a initiates the formation of the recycling endosome from the ERC that carries MHCI back to the PM, nonclathrin recycling endosome (NRE). In the absence of Rab22a, these tubules do not form, the peripheral vesicles are less abundant and MHCI is not efficiently recycled back to the PM.

An interesting contrast to the lack of Rab22a activity described above is the effect of increased Rab22a activity on recycling structures and function. Notable is the increased appearance of tubular MHCI-containing membranes and increased number of MHCI-containing peripheral vesicles in cells expressing Rab22a-Q64L (Figure 5A). However, recycling of MHCI from these structures to the PM is inhibited (Figure 5E), suggesting that Rab22a GTP hydrolysis is required for fusion of these structures back to the PM. Some inhibition of recycling also was observed when the wild-type Rab22a was overexpressed, suggesting that overabundance of Rab22a leads to increased Rab22a-GTP. Overall, it is clear that Rab22a cycling between GTP-bound active and GDP-bound inactive states is required for proper cellular

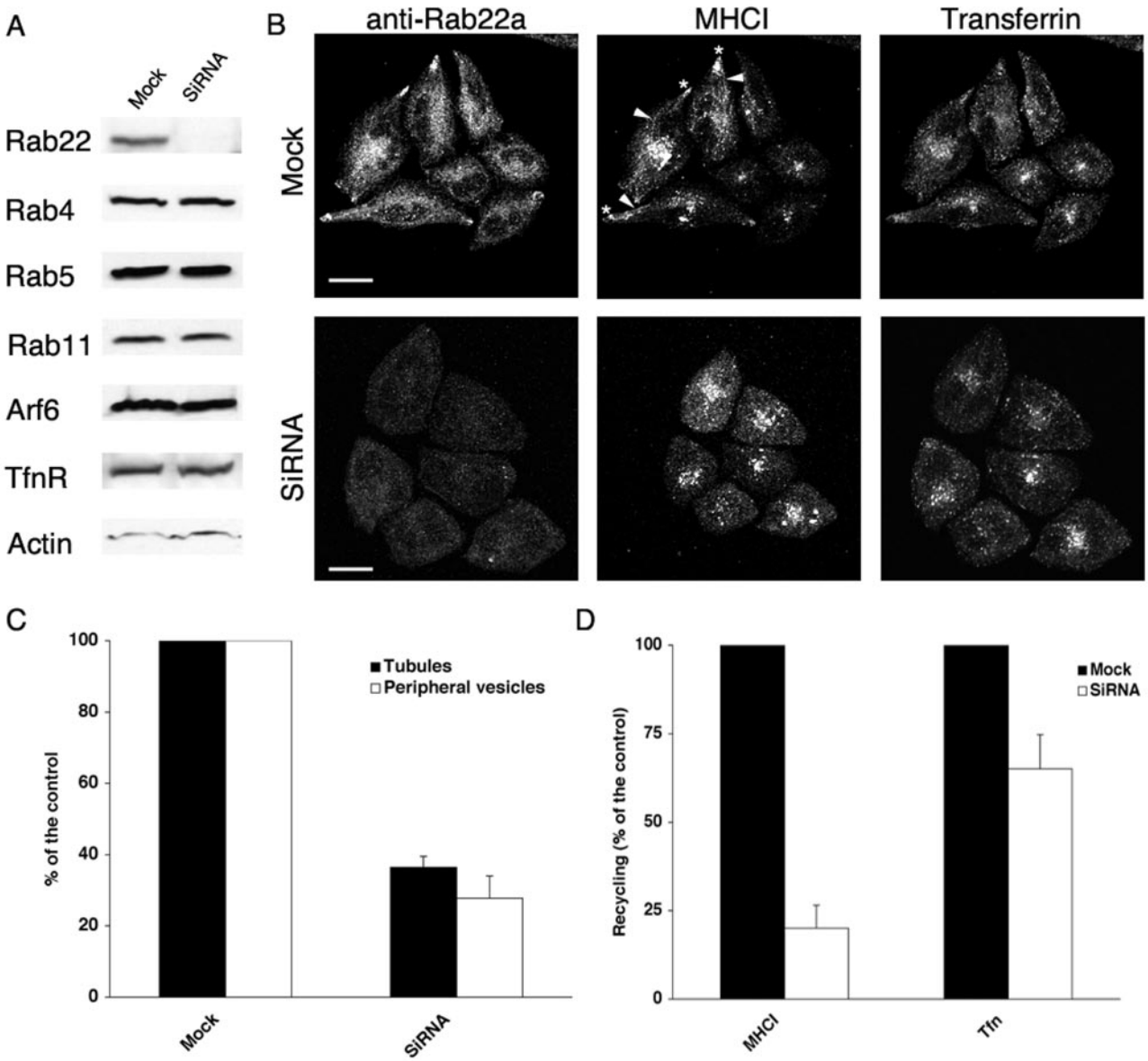

Figure 6. siRNA-mediated depletion of Rab22a inhibits MHCI recycling to the PM. (A) Lysates from either mock- or siRNA-treated cells were subjected to electrophoresis and probed with antibodies directed against Rab22a, Rab4, Rab5, Rab11, Arf6, TfnR, and actin. (B) Mock- (top) or siRNA-treated cells (bottom) were allowed to internalize antibody to MHCI and 633 Tfn and processed for confocal microscopy as described in MATERIALS AND METHODS. Arrowheads and asterisks point to MHCI-containing tubules and MHCI-containing vesicles, respectively. Bars, 10 μm. (C) Mock- or siRNA-treated cells were scored for either MHCI-containing tubules (closed bars) or MHCI-containing vesicles (open bars) as described in MATERIALS AND METHODS. Data are averages of two independent experiments ± SEM. (D) Recycling to the PM of MHCI and Tfn was measured as described in MATERIALS AND METHODS in either mock- (closed bars) or siRNA-treated (open bars) cells. Data are averages of two independent experiments ± SEM. Student's *t*-test was used to test the statistical significance of the data. For the recycling, the p values were mock versus siRNA, $p < 0.001$ for both MHCI and transferrin recycling.

function because both inactive and active mutants of Rab22a inhibit recycling.

Rab22 Works Together with Rab11 to Regulate Recycling of MHCI

Rab11 has been implicated in the regulation of recycling of membrane from the juxtanuclear ERC, most notably in regulating the recycling of transferrin receptor (Ullrich *et al.*, 1996; Volpicelli *et al.*, 2002). Rab11a and b were the only other Rabs that localized with Rab22 on the MHCI-containing, tubular recycling endosomes. Both dominant negative mutant of Rab11a (Figure 7A), and to a lesser extent, Rab11b (our unpublished observations), inhibited the recycling of MHCI back to the PM (Figure 7), as we had observed with Rab22a. This is in agreement with another study showing that the expression of the dominant negative mutant of Rab11a inhibits the serum-stimulated recycling of Integrin β1 (Powelka *et al.*, 2004), a molecule known to traffic with MHCI (Radhakrishna and Donaldson, 1997; Powelka *et al.*, 2004). A remarkable distinction, however, between expression of dominant negative mutants of Rab22a and Rab11 is that the tubular endosomes are not observed with the former

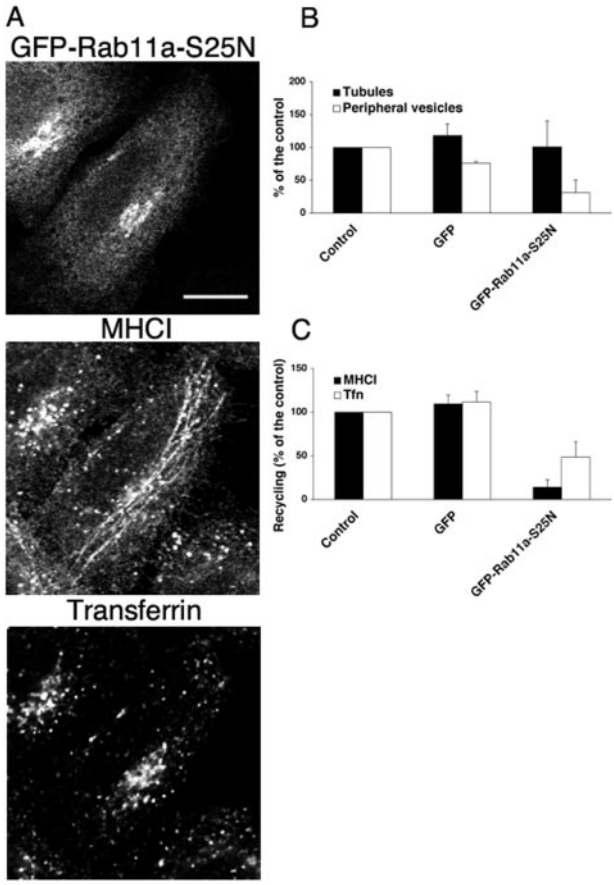

Figure 7. Dominant negative mutant of Rab11a inhibits the recycling to the PM of both MHCI and Tfn. (A) HeLa cells were transfected with GFP-Rab11a-S25N and processed as described in Figure 1. Bars, 10 μm. (B) HeLa cells were transfected as indicated, processed as described in Figure 1 and scored as described in MATERIALS AND METHODS for the presence of MHCI-containing tubules (closed bars) or MHCI-containing peripheral vesicles (open bars). Data are averages of two independent experiments ± the SEM. (C) HeLa cells either nontransfected (control) or transfected as indicated above were allowed to internalize and recycle MHCI (closed bars) or Tfn (open bars) as described in MATERIALS AND METHODS. Recycling of MHCI was measured after 30 min from the release of the LatA block, whereas Tfn recycling was measured after 10 min from the incubation in complete medium. Data, normalized for the control, are averages of two independent experiments ± the SEM. One-way analysis of variance for independent samples was used to test the statistical significance of the data. For control/GFP versus Rab11aS25N, the p values were <0.01 for both MHCI and transferrin recycling.

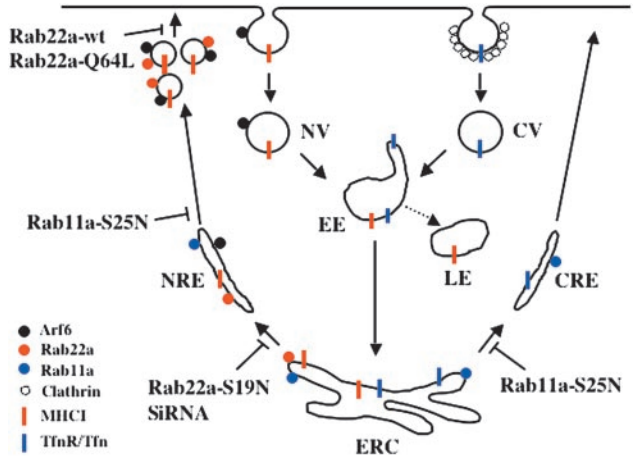

Figure 8. Model depicting the roles of Rab22a and Rab11 in regulating the recycling from the ERC. Nonclathrin-derived cargo (e.g., MHCI) are internalized independently from clathrin-derived cargo (e.g., Tfn and its receptor) in NV as opposed to clathrin vesicles (CV). NV fuse with the EE and from there MHCI is either transported to the late endosome (LE) for the degradation or transported together with TfnR/Tfn (the clathrin cargo) to the juxtanuclear region into the ERC. From the ERC, nonclathrin- and clathrin-derived membrane proteins are sorted in different transport carriers (NRE and CRE, respectively). The activation of Rab22a is required for the formation of the NRE from the ERC, whereas Rab11 acts at a later step possibly in the breakdown of the tubule into vesicles. Finally, inactivation of Rab22a would lead to the fusion of the vesicles to the PM.

as they are with the latter. This suggests that Rab22a activity is critical for the initiation and extension of the tubular membranes from the ERC, the accumulation of vesicles in the periphery, and, upon GTP hydrolysis, the fusion of these vesicles back to the PM. The persistence of tubular endosomes and the absence of peripheral vesicles in cells expressing dominant negative mutants of Rab11 suggest that Rab11 functions not in the formation of tubules, but rather in the accumulation of the peripheral vesicles (Figure 8).

Together, a model emerges that Rab22a and its activation are required to initiate the formation of tubular structures (NRE) from the ERC that move out to the periphery where they might break down into vesicles that then, upon GTP hydrolysis, rapidly fuse with the PM (Figure 8). We think it most likely that these tubules originate from the ERC and not the EE because Rab11 colocalizes to these tubules and Rab4 and Rab5 do not. In addition, Rab11 is required for the recycling, possibly at a site near the PM. Interestingly, coexpression of Rab22a with either Rab11a or b induced the formation of an anastomosing network of tubules that contained both MHCI and transferrin (our unpublished observations), indicating that these two Rab proteins function coordinately.

What might be the role of Rab22a and Rab11? Rab proteins have been implicated in multiple events, including vesicle formation, cargo selection, vesicle transport, and vesicle fusion (Somsel Rodman and Wandinger-Ness, 2000; Segev, 2001; Zerial and McBride, 2001; Miaczynska and Zerial, 2002). Rab22a may be involved initially in sorting and selecting membrane lipid and cargo, such as MHCI- and GPI-anchored proteins, into the forming tubule and its transport out to the periphery. Recent findings that Rab proteins bind to motor proteins to facilitate transport, such as Rab6 with dynactin (Short *et al*., 2002) and Rab27 with myosin V (Wu *et al*., 2002), may be relevant to the functions of Rab22a and Rab11, respectively. The tubular portion of the NRE that carries MHCI back to the PM is aligned along microtubules and because extension of these tubules is Rab22a dependent, it suggests that Rab22a may play a role in attachment to or movement along microtubules. Rab11a and b, on the other hand, have been shown to bind to myosin Vb and influence recycling back to the PM in both polarized and nonpolarized cells (Lapierre *et al*., 2001; Volpicelli *et al*., 2002). Interestingly, recycling of MHCI back to the PM is severely blocked by inhibitors of actin polymerization such as cytochalasin D or LatA (Radhakrishna and Donaldson, 1997; this study) with the result that the tubular NRE accumulates. Thus, it seems possible that Rab22a engages a plus-end directed

microtubule motor to carry it out to the periphery along microtubules and then Rab11 engages a myosin V-type motor to move through the actin network at the cortex to fuse with the PM. Investigations are underway to consider these possibilities.

The Rab22a-associated tubules (NRE) originate from Tfn-containing endosomal structures located in the perinuclear area, most likely the ERC, from which Tfn is believed to recycle (Mayor *et al*., 1993; Lin *et al*., 2002). An intriguing possibility is that in HeLa cells the ERC is a multidomain compartment where MHCI and Tfn receptor are sorted out in different transport intermediates and recycled back to the PM in a process mediated by Rab22a and Rab11. The lack of a total block in recycling when either Rab11 or Rab22a is inhibited might be due to an alternative recycling route from the ERC. In Chinese hamster ovary cells, by contrast, both Tfn- and nonclathrin-derived cargo (e.g., CD59) recycle in the same transport intermediates (Mayor *et al*., 1998), raising the possibility that either the levels or function of Rab22a are altered in Chinese hamster ovary cells. Another interesting aspect of the tubular NRE is the association of Arf6 with these recycling membranes. Arf6 and Rab11 share a common effector, Arfophilin1/FIP3 (Shin *et al*., 2001; Hickson *et al*., 2003), and it will be interesting to see whether Arfophilin functions during the recycling of MHCI.

In summary, we have shown that Rab22a regulates the recycling of cargoes trafficking through the ARF6-associated/clathrin-independent pathway. We propose that the role of Rab22a is to allow the sorting of MHCI-containing membranes from the ERC, their correct delivery to the cell periphery, and their fusion with the plasma membrane.

ACKNOWLEDGMENTS

We thank V. Olkkonen, R. Lodge, J. Cardelli, L. Elferink, J. Goldenring, and P. van der Sluijs for reagents and F. Brown, E. Eisenberg, L. Greene, J. Hammer, E. Korn, and J. Lippincott-Schwartz for critical comments on the manuscript.

REFERENCES

Aderem, A., and Underhill, D.M. (1999). Mechanisms of phagocytosis in macrophages. Annu. Rev. Immunol. *17*, 593–623.

Barbero, P., Bittova, L., and Pfeffer, S.R. (2002). Visualization of Rab9-mediated vesicle transport from endosomes to the trans-Golgi in living cells. J. Cell Biol. *156*, 511–518.

Bonifacino, J.S., and Traub, L.M. (2003). Signals for sorting of transmembrane proteins to endosomes and lysosomes. Annu. Rev. Biochem. *72*, 395–447.

Brown, F.D., Rozelle, A.L., Yin, H.L., Balla, T., and Donaldson, J.G. (2001). Phosphatidylinositol 4,5-bisphosphate and Arf6-regulated membrane traffic. J. Cell Biol. *154*, 1007–1017.

Caplan, S., Naslavsky, N., Hartnell, L.M., Lodge, R., Polishchuk, R.S., Donaldson, J.G., and Bonifacino, J.S. (2002). A tubular EHD1-containing compartment involved in the recycling of major histocompatibility complex class I molecules to the plasma membrane. EMBO J. *21*, 2557–2567.

Chavrier, P., and Goud, B. (1999). The role of ARF and Rab GTPases in membrane transport. Curr. Opin. Cell Biol. *11*, 466–475.

Chimini, G., and Chavrier, P. (2000). Function of Rho family proteins in actin dynamics during phagocytosis and engulfment. Nat. Cell Biol. *2*, E191–E196.

Clague, M.J. (1998). Molecular aspects of the endocytic pathway. Biochem. J. *336*, 271–282.

Conner, S.D., and Schmid, S.L. (2003). Regulated portals of entry into the cell. Nature *422*, 37–44.

de Wit, H., Lichtenstein, Y., Kelly, R.B., Geuze, H.J., Klumperman, J., and van der Sluijs, P. (2001). Rab4 regulates formation of synaptic-like microvesicles from early endosomes in PC12 cells. Mol. Biol. Cell *12*, 3703–3715.

Gruenberg, J., and Maxfield, F.R. (1995). Membrane transport in the endocytic pathway. Curr. Opin. Cell Biol. *7*, 552–563.

Hickson, G.R., Matheson, J., Riggs, B., Maier, V.H., Fielding, A.B., Prekeris, R., Sullivan, W., Barr, F.A., and Gould, G.W. (2003). Arfophilins are dual Arf/Rab 11 binding proteins that regulate recycling endosome distribution and are related to *Drosophila* nuclear fallout. Mol. Biol. Cell *14*, 2908–2920.

Johannes, L., and Lamaze, C. (2002). Clathrin-dependent or not: is it still the question? Traffic *3*, 443–451.

Kauppi, M., Simonsen, A., Bremnes, B., Vieira, A., Callaghan, J., Stenmark, H., and Olkkonen, V.M. (2002). The small GTPase Rab22 interacts with EEA1 and controls endosomal membrane trafficking. J. Cell Sci. *115*, 899–911.

Lapierre, L.A., Kumar, R., Hales, C.M., Navarre, J., Bhartur, S.G., Burnette, J.O., Provance, D.W., Jr., Mercer, J.A., Bahler, M., and Goldenring, J.R. (2001). Myosin Vb is associated with plasma membrane recycling systems. Mol. Biol. Cell *12*, 1843–1857.

Lin, S.X., Gundersen, G.G., and Maxfield, F.R. (2002). Export from pericentriolar endocytic recycling compartment to cell surface depends on stable, detyrosinated (Glu) microtubules and kinesin. Mol. Biol. Cell *13*, 96–109.

Lombardi, D., Soldati, T., Riederer, M.A., Goda, Y., Zerial, M., and Pfeffer, S.R. (1993). Rab9 functions in transport between late endosomes and the trans Golgi network. EMBO J. *12*, 677–682.

Maxfield, F.R., and McGraw, T.E. (2004). Endocytic recycling. Nat. Rev. Mol. Cell. Biol. *5*, 121–132.

Mayor, S., Presley, J.F., and Maxfield, F.R. (1993). Sorting of membrane components from endosomes and subsequent recycling to the cell surface occurs by a bulk flow process. J. Cell Biol. *121*, 1257–1269.

Mayor, S., Sabharanjak, S., and Maxfield, F.R. (1998). Cholesterol-dependent retention of GPI-anchored proteins in endosomes. EMBO J. *17*, 4626–4638.

Mesa, R., Salomon, C., Roggero, M., Stahl, P.D., and Mayorga, L.S. (2001). Rab22a affects the morphology and function of the endocytic pathway. J. Cell Sci. *114*, 4041–4049.

Miaczynska, M., and Zerial, M. (2002). Mosaic organization of the endocytic pathway. Exp. Cell Res. *272*, 8–14.

Naslavsky, N., Weigert, R., and Donaldson, J.G. (2003). Convergence of nonclathrin- and clathrin-derived endosomes involves Arf6 inactivation and changes in phosphoinositides. Mol. Biol. Cell *14*, 417–431.

Naslavsky, N., Weigert, R., and Donaldson, J.G. (2004). Characterization of a non-clathrin pathway: membrane cargo and lipid requirements. Mol. Biol. Cell. *15*, 3520–3529.

Nichols, B.J., and Lippincott-Schwartz, J. (2001). Endocytosis without clathrin coats. Trends Cell Biol. *11*, 406–412.

Nielsen, E., Christoforidis, S., Uttenweiler-Joseph, S., Miaczynska, M., Dewitte, F., Wilm, M., Hoflack, B., and Zerial, M. (2000). Rabenosyn-5, a novel Rab5 effector, is complexed with hVPS45 and recruited to endosomes through a FYVE finger domain. J. Cell Biol. *151*, 601–612.

Pfeffer, S. (2003). Membrane domains in the secretory and endocytic pathways. Cell *112*, 507–517.

Powelka, A.M., Sun, J., Li, J., Gao, M., Shaw, L.M., Sonnenberg, A., and Hsu, V.W. (2004). Stimulation-dependent recycling of integrin beta1 regulated by ARF6 and Rab11. Traffic *5*, 20–36.

Press, B., Feng, Y., Hoflack, B., and Wandinger-Ness, A. (1998). Mutant Rab7 causes the accumulation of cathepsin D and cation-independent mannose 6-phosphate receptor in an early endocytic compartment. J. Cell Biol. *140*, 1075–1089.

Radhakrishna, H., and Donaldson, J.G. (1997). ADP-ribosylation factor 6 regulates a novel plasma membrane recycling pathway. J. Cell Biol. *139*, 49–61.

Rodriguez-Gabin, A.G., Cammer, M., Almazan, G., Charron, M., and Larocca, J.N. (2001). Role of rRAB22b, an oligodendrocyte protein, in regulation of transport of vesicles from trans Golgi to endocytic compartments. J. Neurosci. Res. *66*, 1149–1160.

Schlierf, B., Fey, G.H., Hauber, J., Hocke, G.M., and Rosorius, O. (2000). Rab11b is essential for recycling of transferrin to the plasma membrane. Exp. Cell Res. *259*, 257–265.

Seabra, M.C., Mules, E.H., and Hume, A.N. (2002). Rab GTPases, intracellular traffic and disease. Trends Mol. Med. *8*, 23–30.

Segev, N. (2001). Ypt and Rab GTPases: insight into functions through novel interactions. Curr. Opin. Cell Biol. *13*, 500–511.

Shin, O.H., Couvillon, A.D., and Exton, J.H. (2001). Arfophilin is a common target of both class II and class III ADP-ribosylation factors. Biochemistry *40*, 10846–10852.

Short, B., Preisinger, C., Schaletzky, J., Kopajtich, R., and Barr, F.A. (2002). The Rab6 GTPase regulates recruitment of the dynactin complex to Golgi membranes. Curr. Biol. *12*, 1792–1795.

Somsel Rodman, J., and Wandinger-Ness, A. (2000). Rab GTPases coordinate endocytosis. J. Cell Sci. *113*, 183–192.

Song, J., Khachikian, Z., Radhakrishna, H., and Donaldson, J.G. (1998). Localization of endogenous ARF6 to sites of cortical actin rearrangement and involvement of ARF6 in cell spreading. J. Cell Sci. *111*, 2257–2267.

Sonnichsen, B., De Renzis, S., Nielsen, E., Rietdorf, J., and Zerial, M. (2000). Distinct membrane domains on endosomes in the recycling pathway visualized by multicolor imaging of Rab4, Rab5, and Rab11. J. Cell Biol. *149*, 901–914.

Ullrich, O., Reinsch, S., Urbe, S., Zerial, M., and Parton, R.G. (1996). Rab11 regulates recycling through the pericentriolar recycling endosome. J. Cell Biol. *135*, 913–924.

van der Sluijs, P., Hull, M., Webster, P., Male, P., Goud, B., and Mellman, I. (1992). The small GTP-binding protein rab4 controls an early sorting event on the endocytic pathway. Cell *70*, 729–740.

Volpicelli, L.A., Lah, J.J., Fang, G., Goldenring, J.R., and Levey, A.I. (2002). Rab11a and myosin Vb regulate recycling of the M4 muscarinic acetylcholine receptor. J. Neurosci. *22*, 9776–9784.

Watts, C. (1997). Capture and processing of exogenous antigens for presentation on MHC molecules. Annu. Rev. Immunol. *15*, 821–850.

Wu, X., Wang, F., Rao, K., Sellers, J.R., and Hammer, J.A., 3rd. (2002). Rab27a is an essential component of melanosome receptor for myosin Va. Mol. Biol. Cell *13*, 1735–1749.

Zerial, M., and McBride, H. (2001). Rab proteins as membrane organizers. Nat. Rev. Mol. Cell. Biol. *2*, 107–117.

Zuk, P.A., and Elferink, L.A. (2000). Rab15 differentially regulates early endocytic trafficking. J. Biol. Chem. *275*, 26754–26764.